


Equilibration of kinetic temperatures in face-centered cubic latticesVitaly A. Kuzkin^{1,2} and Sergei D. Liazhkov¹¹*Peter the Great Saint Petersburg Polytechnical University, Saint Petersburg, Russia*²*Institute for Problems in Mechanical Engineering RAS, Saint Petersburg, Russia* (Received 29 May 2020; revised 3 September 2020; accepted 2 October 2020; published 28 October 2020)

We study thermal equilibration in face-centered cubic lattices with harmonic and anharmonic (Lennard-Jones) interactions. Initial conditions are chosen such that the kinetic temperatures, corresponding to three spatial directions, are different. We show that in the anharmonic case the approach to thermal equilibrium has two time scales. The first time scale is the period of atomic vibration. At times of the order of several atomic periods, the approach to equilibrium is accompanied by decaying high frequency oscillations of the temperatures. The oscillations are described analytically using the harmonic approximation. In particular, the characteristic frequencies of the oscillations are calculated. It is shown that the oscillations decay in time more slowly than expected. The second time scale, presented in the anharmonic case only, depends on the initial temperature of the system. Normalizing time by this scale, we obtain numerically a universal curve describing equilibration in the Lennard-Jones crystal over a wide range of temperatures.

DOI: [10.1103/PhysRevE.102.042219](https://doi.org/10.1103/PhysRevE.102.042219)**I. INTRODUCTION**

The concept of kinetic temperature as a single scalar parameter, characterizing the thermal state of a system, works well at (or close to) a thermal equilibrium. Far from the thermal equilibrium, the kinetic energies, corresponding to various degrees of freedom, may be different and therefore several kinetic temperatures are introduced [1–13]. For example, solids under laser excitation have two distinct temperatures, corresponding to lattice and electronic subsystems [2,3]. In shock waves, the kinetic temperatures, corresponding to the motion of particles along and across the front, are different [4–10]. Multiple temperatures are also observed during steady [12] and unsteady [13] ballistic heat transport in diatomic chains. In the present paper, we address the question of how these temperatures equilibrate after excitation.

After external excitation, systems tend toward a thermal equilibrium. This approach to the thermal equilibrium is accompanied by changes in the kinetic temperatures. In this paper we focus on two physical processes, responsible for these changes, namely redistribution of the total energy among kinetic and potential forms and redistribution of the kinetic energy among degrees of freedom. In the harmonic approximation, these processes may be described analytically. For example, in the pioneering work of Klein and Prigogine [14], thermal equilibration is investigated in a monoatomic harmonic one-dimensional chain with random initial conditions. It was shown that oscillations of the kinetic and potential energies of the chain are described by the Bessel function. This result was also obtained by entirely different means in Ref. [15], while a theory describing thermal equilibration in the harmonic approximation is developed in Refs. [15–22]. This theory has been successfully applied to

various one-dimensional [15,16,20,21] and two-dimensional [17,19,22] lattices.

In spite of significant progress in the analytical description of the thermal equilibration in harmonic crystals, many questions remain open. In particular, theory predicts that equilibration is accompanied by oscillations of the kinetic temperatures. Calculation of the characteristic frequencies of these oscillations is not straightforward even for simple two-dimensional lattices [23]. Therefore, in the present paper we present a simple numerical procedure for calculation of these frequencies, based on the Fourier transform. Another open question is the decay rate of temperature oscillations. In principle, the decay rate may be calculated by the stationary phase method [24,25]. This method predicts that in the d -dimensional case the oscillations decay in time as $t^{-d/2}$, provided that the dispersion relation contains no degenerate stationary points.¹ This simple power law is satisfied for many lattices [15–17,19]. However, we show below that for the face-centered cubic (fcc) lattice this is not the case.

The description of thermal equilibration in anharmonic crystals is even more challenging. At short times, the equilibration can be described using the harmonic approximation with reasonable accuracy [17,26]. At large times, however, the harmonic approximation is inapplicable. In particular, the harmonic theory predicts generally different equilibrium values for the kinetic temperatures [19], while in the anharmonic crystals they are equal. The mechanism, leading to the equalization of the temperatures, is the exchange of energy

¹The stationary point is the point in the wave-vector space, corresponding to zero group velocity. It is called degenerate if Hessian of the dispersion relation at this point is equal to zero (see, e.g., Refs. [24,25]).

among normal modes of the system [27]. In the literature, this mechanism is intensively studied in the context of the Fermi-Pasta-Ulam-Tsingou (FPUT) problem [28]. The current status of solution of the FPUT problem is summarized in Refs. [26,29–34]. In particular, in Ref. [26] it has been shown that the FPUT recurrence paradox is eliminated at finite temperatures. However, in spite of significant progress in the solution of the FPUT problem, a comprehensive theory, describing the exchange of energy among the normal modes and therefore equalization of the temperatures in the anharmonic crystals, has yet to be developed.

We also mention Ref. [17], where the equilibration of temperatures in the two-dimensional Lennard-Jones crystal was studied numerically. It was shown that in the anharmonic case equilibration is faster at higher temperatures. The existence of an additional time scale, determined by anharmonic effects, was also demonstrated. However, the temperature dependence of this time scale was not studied. Therefore, we address this important issue below.

In this paper, we report results on the equilibration of kinetic temperatures, corresponding to three spatial directions in fcc lattices with harmonic and anharmonic interactions. We show that in the anharmonic case the approach to thermal equilibrium has two time scales. At the first (small) time scale, the equilibration is accompanied by decaying high frequency oscillations of the kinetic temperatures. Frequencies and decay rates of these oscillations are calculated using the harmonic approximation. At the second (large) time scale, the temperatures tend to equilibrium values. The temperature dependence of this time scale is calculated using molecular dynamics simulations. A universal curve describing the equilibration at different initial temperatures is then obtained.

II. EQUATIONS OF MOTION AND INITIAL CONDITIONS

In this section, we formulate equations of motion and initial conditions for the harmonic fcc lattice. The initial conditions are chosen such that the kinetic temperatures, corresponding to three spatial directions, are different.

We consider an infinite harmonic crystal possessing an fcc lattice, consisting of identical particles. Each particle interacts with its 12 nearest neighbors, numbered by index α . Vectors, connecting a particle with its neighbors, are denoted by \mathbf{a}_α ,² $\alpha = 0, \pm 1, \dots, \pm 6$. Obviously $\mathbf{a}_0 = 0$. Corresponding unit vectors $\mathbf{n}_\alpha = \mathbf{a}_\alpha/|\mathbf{a}_\alpha|$ are given by

$$\begin{aligned} \mathbf{n}_1 &= (\mathbf{e}_x + \mathbf{e}_y)/\sqrt{2}, & \mathbf{n}_4 &= \mathbf{n}_3 - \mathbf{n}_2, \\ \mathbf{n}_2 &= (\mathbf{e}_y + \mathbf{e}_z)/\sqrt{2}, & \mathbf{n}_5 &= \mathbf{n}_1 - \mathbf{n}_3, \\ \mathbf{n}_3 &= (\mathbf{e}_x + \mathbf{e}_z)/\sqrt{2}, & \mathbf{n}_6 &= \mathbf{n}_1 - \mathbf{n}_2, \\ \mathbf{n}_\alpha &= -\mathbf{n}_{-\alpha}, \end{aligned} \quad (1)$$

where $\mathbf{e}_x, \mathbf{e}_y, \mathbf{e}_z$ are Cartesian unit vectors, directed along the axes of cubic symmetry [35]. The position vector, \mathbf{x} , of a particle is represented by

$$\mathbf{x} = a(A_1\mathbf{n}_1 + A_2\mathbf{n}_2 + A_3\mathbf{n}_3), \quad (2)$$

where a is the lattice constant; A_1, A_2, A_3 are integers.

The neighboring particles are connected by linear springs. The equation of motion for the particle, \mathbf{x} , is written as

$$m\ddot{\mathbf{u}}(\mathbf{x}) = \sum_{\alpha} \mathbf{C}_\alpha \mathbf{u}(\mathbf{x} + \mathbf{a}_\alpha), \quad (3)$$

where $\mathbf{u}(\mathbf{x}) = (u_x, u_y, u_z)^\top$ is a column vector, consisting of the components of displacements; \top stands for the transpose sign. The matrices \mathbf{C}_α for the fcc lattice are given by

$$\begin{aligned} \mathbf{C}_1 &= \mathbf{C}_{-1} = \frac{c}{2} \begin{pmatrix} 1 & 1 & 0 \\ 1 & 1 & 0 \\ 0 & 0 & 0 \end{pmatrix}, \\ \mathbf{C}_2 &= \mathbf{C}_{-2} = \frac{c}{2} \begin{pmatrix} 0 & 0 & 0 \\ 0 & 1 & 1 \\ 0 & 1 & 1 \end{pmatrix}, \\ \mathbf{C}_3 &= \mathbf{C}_{-3} = \frac{c}{2} \begin{pmatrix} 1 & 0 & 1 \\ 0 & 0 & 0 \\ 1 & 0 & 1 \end{pmatrix}, \\ \mathbf{C}_4 &= \mathbf{C}_{-4} = \frac{c}{2} \begin{pmatrix} 1 & -1 & 0 \\ -1 & 1 & 0 \\ 0 & 0 & 0 \end{pmatrix}, \\ \mathbf{C}_5 &= \mathbf{C}_{-5} = \frac{c}{2} \begin{pmatrix} 0 & 0 & 0 \\ 0 & 1 & -1 \\ 0 & -1 & 1 \end{pmatrix}, \\ \mathbf{C}_6 &= \mathbf{C}_{-6} = \frac{c}{2} \begin{pmatrix} 1 & 0 & -1 \\ 0 & 0 & 0 \\ -1 & 0 & 1 \end{pmatrix}, \\ \mathbf{C}_0 &= -4c\mathbf{I}, \end{aligned} \quad (4)$$

where c is the bond stiffness; \mathbf{I} is the 3×3 identity matrix. Note that matrices \mathbf{C}_α are symmetric.

We consider the following initial conditions for particles, corresponding to a uniform spatial distribution of kinetic temperatures in the crystal:

$$\begin{aligned} u_x &= u_y = u_z = 0, & \dot{u}_x &= \beta_x(\mathbf{x})\sqrt{k_B T_{xx}^0/m}, \\ \dot{u}_y &= \beta_y(\mathbf{x})\sqrt{k_B T_{yy}^0/m}, & \dot{u}_z &= \beta_z(\mathbf{x})\sqrt{k_B T_{zz}^0/m}, \end{aligned} \quad (5)$$

where k_B is the Boltzmann constant; $T_{xx}^0, T_{yy}^0, T_{zz}^0$ are initial kinetic temperatures, corresponding to spatial directions x, y, z [see definition (11)]; $\beta_x(\mathbf{x}), \beta_y(\mathbf{x}), \beta_z(\mathbf{x})$ are uncorrelated random values with zero mathematical expectation and unit variance,³ i.e., $\langle \beta_x(\mathbf{x}) \rangle = \langle \beta_y(\mathbf{x}) \rangle = \langle \beta_z(\mathbf{x}) \rangle = 0$, $\langle \beta_x(\mathbf{x})^2 \rangle = \langle \beta_y(\mathbf{x})^2 \rangle = \langle \beta_z(\mathbf{x})^2 \rangle = 1$, and $\langle \beta_x(\mathbf{x})\beta_y(\mathbf{y}) \rangle = \langle \beta_x(\mathbf{x})\beta_z(\mathbf{y}) \rangle = 0$. The case of a spatially nonuniform distribution of initial temperatures is discussed in Sec. VI.

In the next section, the dispersion relation, corresponding to (3), is derived for further analysis of thermal equilibration.

III. DISPERSION RELATION

In Refs. [18,19], it has been shown that the dispersion relation is required to describe thermal equilibration in the

²Here and below, invariant vectors (e.g., position vector) are denoted by bold symbols. Matrices are denoted by bold italic symbols.

³In numerical simulations, uniform distribution of the random values $\beta_x, \beta_y, \beta_z$ in formula (5) is used.

harmonic approximation. To obtain the dispersion relation $\omega(\mathbf{k})$, we seek a solution of (3) in the form

$$\begin{aligned} \mathbf{u}(\mathbf{x}) &= \mathbf{A} e^{i(\omega t + \mathbf{k} \cdot \mathbf{x})}, \quad i^2 = -1, \\ \mathbf{k} &= (\theta_1 \hat{\mathbf{n}}_1 + \theta_2 \hat{\mathbf{n}}_2 + \theta_3 \hat{\mathbf{n}}_3)/a, \end{aligned} \quad (6)$$

where \mathbf{A} is a constant column vector; \mathbf{k} is the wave vector; $\theta_1, \theta_2, \theta_3 \in [0; 2\pi]$; $\hat{\mathbf{n}}_1, \hat{\mathbf{n}}_2, \hat{\mathbf{n}}_3$ are vectors of a reciprocal basis such that $\hat{\mathbf{n}}_i \cdot \hat{\mathbf{n}}_j = \delta_{ij}$, where δ_{ij} is the Kronecker delta.

Substituting (6) into (3), we obtain a homogeneous system of linear equations

$$(\boldsymbol{\Omega} - \omega^2 \mathbf{I})\mathbf{A} = \mathbf{0}, \quad \boldsymbol{\Omega} = -\frac{1}{m} \sum_{\alpha} \mathbf{C}_{\alpha} e^{i\mathbf{k} \cdot \mathbf{a}_{\alpha}}, \quad (7)$$

where $\boldsymbol{\Omega}$ is the dynamical matrix of the lattice. Substitution of expressions (4) for matrices \mathbf{C}_{α} into (7) yields

$$\begin{aligned} \Omega_{11} &= f(\theta_1, \theta_3, \theta_2), & \Omega_{12} &= \Omega_{21} = g(\theta_1, \theta_3, \theta_2), \\ \Omega_{13} &= \Omega_{31} = g(\theta_3, \theta_2, \theta_1), & \Omega_{22} &= f(\theta_2, \theta_1, \theta_3), \\ \Omega_{23} &= \Omega_{32} = g(\theta_2, \theta_1, \theta_3), & \Omega_{33} &= f(\theta_3, \theta_2, \theta_1), \\ f(\theta_1, \theta_2, \theta_3) &= 2\omega_e^2 \left(\sin^2 \frac{\theta_1}{2} + \sin^2 \frac{\theta_1 - \theta_3}{2} + \sin^2 \frac{\theta_2}{2} \right. \\ &\quad \left. + \sin^2 \frac{\theta_2 - \theta_3}{2} \right), \\ g(\theta_1, \theta_2, \theta_3) &= 2\omega_e^2 \left(\sin^2 \frac{\theta_1}{2} - \sin^2 \frac{\theta_2 - \theta_3}{2} \right), \quad \omega_e^2 = \frac{c}{m}. \end{aligned} \quad (8)$$

These formulas show that the matrix $\boldsymbol{\Omega}$ is real and symmetric. It can be therefore represented as

$$\boldsymbol{\Omega} = \mathbf{P} \boldsymbol{\Lambda} \mathbf{P}^{\top}, \quad \Lambda_{ij} = \omega_j^2 \delta_{ij}, \quad (9)$$

where ω_j^2 are eigenvalues of $\boldsymbol{\Omega}$; ω_j , $j = 1, 2, 3$, are branches of the dispersion relation for the lattice; \mathbf{P} is an orthogonal matrix, composed of the unit eigenvectors of the dynamical matrix $\boldsymbol{\Omega}$. Note that all branches of the dispersion relation are symmetric with respect to a permutation of any two components of the wave vector, i.e., $\omega_j(\theta_1, \theta_2, \theta_3) = \omega_j(\theta_3, \theta_2, \theta_1) = \omega_j(\theta_2, \theta_1, \theta_3)$, etc.

Thus the dispersion relation is represented via eigenvalues of the dynamical matrix. In the next section, the dispersion relation is employed in the description of transient thermal processes.

IV. THERMAL EQUILIBRATION (HARMONIC APPROXIMATION)

Initial conditions (5) specify finite kinetic energy and zero excess potential energy. The motion of particles leads to equilibration of kinetic and potential energies and partial redistribution of the energy among the degrees of freedom. These transient processes cause high frequency oscillations of the kinetic temperatures, corresponding to the spatial directions x, y, z . In this section, we present an analytical solution describing these oscillations in the harmonic approximation, and calculate decay rates and characteristic frequencies of these oscillations.

A. Analytical solution

To define the kinetic temperatures, we consider an infinite number of realizations of the same crystal, which differ

only by random initial conditions (5). According to (5), the initial kinetic temperatures, corresponding to different spatial directions, are generally not equal. Therefore, to describe the thermal state of a crystal, the temperature matrix, \mathbf{T} , is introduced [19]:

$$k_B \mathbf{T} = m \begin{pmatrix} \langle \dot{u}_x^2 \rangle & \langle \dot{u}_x \dot{u}_y \rangle & \langle \dot{u}_x \dot{u}_z \rangle \\ \langle \dot{u}_x \dot{u}_y \rangle & \langle \dot{u}_y^2 \rangle & \langle \dot{u}_y \dot{u}_z \rangle \\ \langle \dot{u}_x \dot{u}_z \rangle & \langle \dot{u}_y \dot{u}_z \rangle & \langle \dot{u}_z^2 \rangle \end{pmatrix}. \quad (10)$$

In numerical simulations, the mathematical expectation indicated by $\langle \dots \rangle$ in (10) may be replaced either by one or both of averaging over realizations or particles. The corresponding results coincide when the numbers of particles and realizations tend to infinity.

The diagonal elements of the temperature matrix are proportional to the kinetic temperatures, corresponding to the three spatial directions

$$k_B T_{xx} = m \langle \dot{u}_x^2 \rangle, \quad k_B T_{yy} = m \langle \dot{u}_y^2 \rangle, \quad k_B T_{zz} = m \langle \dot{u}_z^2 \rangle. \quad (11)$$

The off-diagonal elements are proportional to correlations between components of the velocity.

We use the following exact formula, describing the evolution over time of the temperature matrix [19]:

$$\mathbf{T} = \frac{1}{2} \int_{\mathbf{k}} \mathbf{P} \tilde{\mathbf{T}} \mathbf{P}^{\top} d\mathbf{k},$$

$$\tilde{T}_{ij} = \{ \mathbf{P}^{\top} \mathbf{T}_0 \mathbf{P} \}_{ij} [\cos((\omega_i - \omega_j)t) + \cos((\omega_i + \omega_j)t)],$$

$$\int_{\mathbf{k}} \dots d\mathbf{k} = \frac{1}{8\pi^3} \int_0^{2\pi} \int_0^{2\pi} \int_0^{2\pi} \dots d\theta_1 d\theta_2 d\theta_3, \quad (12)$$

where \mathbf{T}_0 is the initial value of the temperature matrix; $\{ \dots \}_{ij}$ is the element i, j of the matrix; \mathbf{P} is defined by (9). We also consider the average kinetic temperature

$$T = \text{tr} \mathbf{T} / 3 = (T_{xx} + T_{yy} + T_{zz}) / 3,$$

which is proportional to the total kinetic energy of the system.

Calculation of the trace in (12) yields the following expression for the average kinetic temperature:

$$\begin{aligned} T &= \frac{T_0}{2} + \frac{T_0}{6} \sum_{j=1}^3 \int_{\mathbf{k}} \cos(2\omega_j(\mathbf{k})t) d\mathbf{k} \\ &\quad + \frac{1}{6} \int_{\mathbf{k}} \sum_{j=1}^3 \{ \mathbf{P}^{\top} \text{dev} \mathbf{T}_0 \mathbf{P} \}_{jj} \cos(2\omega_j(\mathbf{k})t) d\mathbf{k}, \end{aligned} \quad (13)$$

where $T_0 = \text{tr} \mathbf{T}_0 / 3$ is the average kinetic temperature; $\text{dev} \mathbf{T}_0$ is the deviator of the initial temperature matrix. Analysis of (13) shows that the third term is equal to zero. Therefore, the initial distribution of temperature among the spatial directions has no influence on oscillations of the average kinetic temperature

$$T = \frac{T_0}{2} + T_1 + T_2 + T_3, \quad T_j = \frac{T_0}{6} \int_{\mathbf{k}} \cos(2\omega_j(\mathbf{k})t) d\mathbf{k}. \quad (14)$$

Here, T_j are the contributions of branches of the dispersion relation to the oscillations of the average kinetic temperature (see Fig. 3). The characteristic frequencies and decay rates of these oscillations are calculated below.

Eventually, the system tends to a state wherein the temperatures are constant in time. This state is henceforth referred to as the thermal equilibrium. Since in harmonic crystals there is no energy exchange among the normal modes, the classical equipartition theorem, predicting equal equilibrium temperatures, is inapplicable. In the harmonic case, these equilibrium values are different and dependent on the initial conditions (see Fig. 2). Therefore, we use the following formula, referred to as the nonequipartition theorem [19]:

$$T_{eq} = \frac{1}{6} \text{tr}(\mathbf{T}_0) \mathbf{I} + \frac{1}{2} \int_{\mathbf{k}} \mathbf{P} \text{diag}(\mathbf{P}^\top \text{dev } \mathbf{T}_0 \mathbf{P}) \mathbf{P}^\top d\mathbf{k}, \quad (15)$$

where $\text{diag}(\dots)$ yields the diagonal part of the matrix. The theorem relates the equilibrium values of temperatures T_{xx} , T_{yy} , T_{zz} to the initial conditions (matrix \mathbf{T}_0).

The approach to the thermal equilibrium in the harmonic fcc lattice is thus described analytically by (12), (14), and (15). The formulas describe oscillations of the kinetic temperatures caused by equilibration of kinetic and potential energies and redistribution of the energy among spatial directions. The characteristic time scale of these oscillations is determined by the atomic period $\tau_e = 2\pi \sqrt{m/c}$.

B. Comparison with a numerical solution

In this subsection, we compare the predictions of formulas (12), (14), and (15), describing the behaviors of the temperatures, with a numerical solution of the initial value problem (3) and (5), where $T_{xx}^0 \neq 0$ and $T_{yy}^0 = T_{zz}^0 = 0$.

The numerical integration is carried out using the symplectic leap-frog scheme with a time step equal to $10^{-2}\tau_e$. In simulations, the lattice consists of 72^3 particles under periodic boundary conditions. Numerical results are averaged over 60 realizations with random initial conditions (5). The integrals in (12), (14), and (15) are calculated numerically using the Riemann sum approximation, where the integration domain is divided into 10^8 equal cubes.

Oscillations of the average kinetic temperature T , caused by equilibration of kinetic and potential energies in the harmonic fcc lattice, are presented in Fig. 1. It can be seen that analytical and numerical solutions practically coincide.

An analysis of (12) shows that $T_{zz} = T_{yy}$. Therefore, we consider below only T_{xx} and T_{yy} . Time evolution of the difference of the kinetic temperatures $T_{xx} - T_{yy}$ is shown in Fig. 2. The difference tends to the equilibrium value $0.21T_0$, as predicted by the nonequipartition theorem (15).

Thus formulas (12), (14), and (15) accurately describe thermal equilibration in the harmonic fcc lattice. The formulas have a single characteristic time scale, which is equal to the atomic period τ_e . In Sec. V, we show numerically that the presented harmonic theory is also valid in anharmonic lattices at short times (low temperatures).

C. Characteristic frequencies and decay rates of temperature oscillations

In this subsection, we calculate the characteristic frequencies and decay rates of the temperature oscillations. To simplify the analysis of temperature oscillations, we consider the individual contributions T_1 , T_2 , T_3 of branches of the dispersion relation separately. The contributions, calcu-

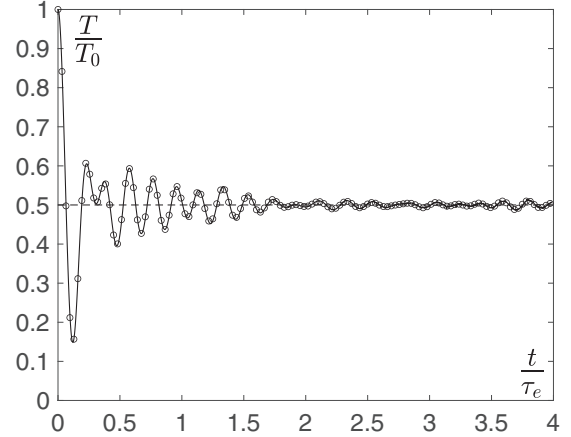


FIG. 1. Oscillations of the average kinetic temperature, T , in the harmonic fcc lattice with random initial velocities. The analytical solution [solid line, Eq. (14)] and numerical solution of the lattice dynamics equations in the harmonic approximation (circles) are shown.

lated by (14), are presented in Fig. 3. In principle, the decay rates and frequencies of temperature oscillations may be obtained by the asymptotic analysis of the integrals (14) by the stationary phase method [24,25]. However, this analysis is rather cumbersome even in the two-dimensional case (see, e.g., Ref. [23]). Therefore, we will use a simple numerical approach.

We estimate the decay rates of the oscillations, given by T_1 , T_2 , and T_3 , as follows. Multiplication of T_2 and T_3 by $t^{\frac{3}{2}}$ yields nondecaying oscillations. Then T_2 and T_3 indeed decay as $1/t^{\frac{3}{2}}$. In contrast, amplitude of oscillations described by the function $t^{\frac{3}{2}}T_1$ grows in time. Therefore, T_1 decays more slowly than $t^{\frac{3}{2}}$. Using a trial and error approach, we have shown numerically that T_1 decays approximately like $1/t$. A possible explanation for this slow decay is presented below.

The frequencies of the temperature oscillations are calculated using formula (14) and the discrete Fourier transform. We introduce dimensionless complex-valued functions \mathcal{F}_i

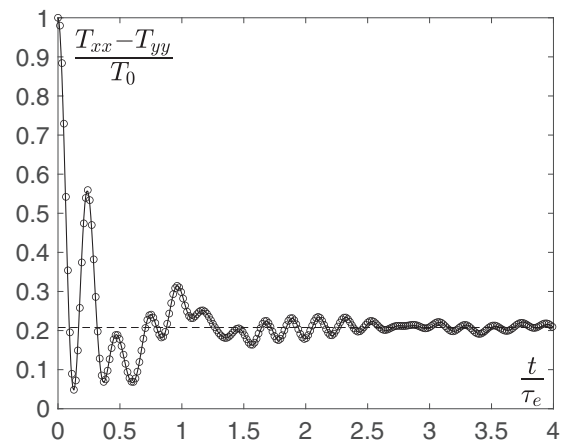


FIG. 2. Redistribution of kinetic energy (temperature) among x and y directions in the harmonic fcc lattice. The analytical solution (12) (solid line), numerical solution of the lattice dynamics equations (3) (circles), and the equilibrium value (15) (dashed line) are shown.

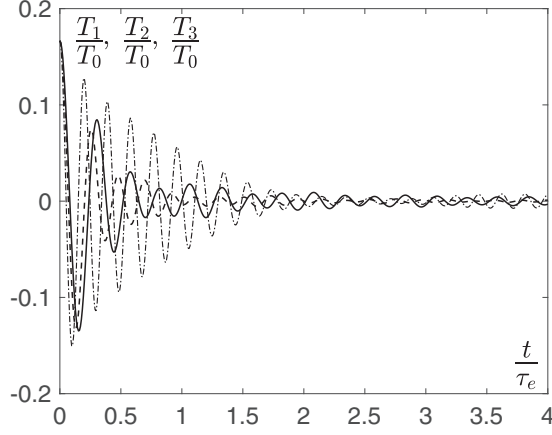


FIG. 3. Contributions of the branches of the dispersion relation to oscillations of the average kinetic temperature. The quantities T_1 (solid line), T_2 (dashed line), and T_3 (dash-dotted line), defined by formula (14), are shown.

such that

$$\begin{aligned} \mathcal{F}_1 &= \Phi(T_1 \omega_e t / T_0), & \mathcal{F}_2 &= \Phi\left(T_2 \omega_e^{\frac{3}{2}} t^{\frac{3}{2}} / T_0\right), \\ \mathcal{F}_3 &= \Phi\left(T_3 \omega_e^{\frac{3}{2}} t^{\frac{3}{2}} / T_0\right), & \Phi(f(t)) &= \sum_{j=0}^{N_t-1} f(t_j) e^{-i\mathcal{W}(k)t_j}, \\ \mathcal{W}(k) &= 2\pi k / (N_t \Delta t), & t_j &= j \Delta t. \end{aligned} \quad (16)$$

In our calculations, $N_t = 500$ and $\Delta t = 0.02\tau_e$. The positions of the local maxima of $|\mathcal{F}_j| = \sqrt{\text{Re}(\mathcal{F}_j)^2 + \text{Im}(\mathcal{F}_j)^2}$ determine the frequencies of the temperature oscillations. Functions $|\mathcal{F}_j|$, calculated using the analytical solution (14), are shown in Fig. 4. It can be seen that the $|\mathcal{F}_j|$ have local maxima at frequencies

$$\begin{aligned} \mathcal{W}_1/\omega_e &\approx 1.41 \pm 0.03, & \mathcal{W}_2/\omega_e &\approx 1.99 \pm 0.03, \\ \mathcal{W}_3/\omega_e &\approx 2.44 \pm 0.03, & \mathcal{W}_4/\omega_e &\approx 2.50 \pm 0.03, \\ \mathcal{W}_5/\omega_e &\approx 2.66 \pm 0.03, & \mathcal{W}_6/\omega_e &\approx 2.82 \pm 0.03. \end{aligned} \quad (17)$$

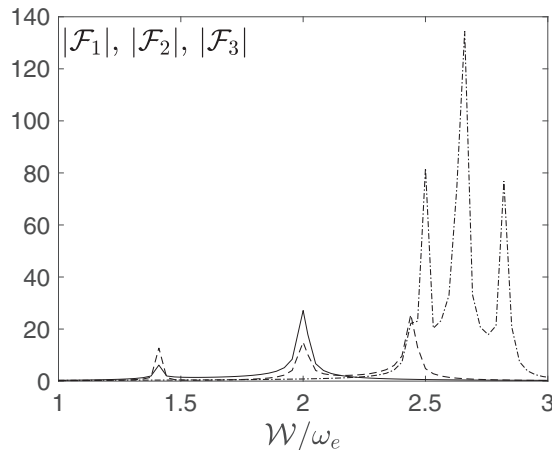


FIG. 4. Functions $|\mathcal{F}_j|$, defined by (16) [$|\mathcal{F}_1|$ (solid line), $|\mathcal{F}_2|$ (dashed line), and $|\mathcal{F}_3|$ (dash-dotted line)].

Here $\mathcal{W}_1, \mathcal{W}_2$ are characteristic frequencies, corresponding to the contribution of the first branch, T_1 ; $\mathcal{W}_1, \mathcal{W}_2, \mathcal{W}_3$ —of the second branch T_2 ; $\mathcal{W}_4, \mathcal{W}_5, \mathcal{W}_6$ —of the third branch T_3 . Some of these frequencies coincide with maxima of the branches, specifically

$$\begin{aligned} \mathcal{W}_2 &\approx \max_{\mathbf{k}} \omega_1 = 2\omega_e, & \mathcal{W}_3 &\approx \max_{\mathbf{k}} \omega_2 = \sqrt{6}\omega_e, \\ \mathcal{W}_6 &\approx \max_{\mathbf{k}} \omega_3 = 2\sqrt{2}\omega_e. \end{aligned} \quad (18)$$

From the stationary phase method [24] it follows that the characteristic frequencies of the temperature oscillations may correspond to zeros of the group velocities. To check this statement, we calculate the frequencies, corresponding to $\mathbf{v}_j^g = 0$, using the definition

$$\mathbf{v}_j^g = a \frac{d\omega_j}{d\mathbf{k}} = a \sum_{i=1}^3 v_{ji}^g \mathbf{n}_i, \quad v_{ji}^g = \frac{\partial \omega_j}{\partial \theta_i}. \quad (19)$$

Our calculations show that $\mathbf{v}_1^g = 0$ for $\omega_1 = \mathcal{W}_1$, $\omega_1 = \mathcal{W}_2$, $\mathbf{v}_2^g = 0$ for $\omega_2 = \mathcal{W}_1$, $\omega_2 = \mathcal{W}_2$, and $\mathbf{v}_3^g = 0$ for $\omega_3 = \mathcal{W}_4$, $\omega_3 = \mathcal{W}_5$, $\omega_3 = \mathcal{W}_6$. Then, all the frequencies (17), except for \mathcal{W}_3 , correspond to zero group velocities. For $\omega_2 = \mathcal{W}_3$ the group velocity \mathbf{v}_2^g is discontinuous.

Thus oscillations of the kinetic temperature T have six different characteristic frequencies (17). Five of these correspond to zero group velocities, while \mathcal{W}_3 corresponds to a discontinuity in the group velocity. The oscillations decay more slowly than $1/t^{\frac{3}{2}}$ (approximately like $1/t$). This slow decay may be due to the fact that the dispersion relation has zero Hessian at $\omega_1 = \mathcal{W}_2$. However, since no general analytical results are available for this degenerate case [25], more detailed analysis of the asymptotic behavior is required. This analysis is beyond the scope of the present paper.

V. THERMAL EQUILIBRATION IN A LENNARD-JONES CRYSTAL

In this section, we investigate the influence of nonlinearity of interatomic interactions on equilibration of the kinetic temperatures T_{xx}, T_{yy} . We show that, in the anharmonic case, approach to thermal equilibrium has a second time scale, depending on the initial temperature.

A. Numerical results

We consider the fcc lattice with interparticle interactions described by the Lennard-Jones potential

$$\Pi(r) = \varepsilon \left[\left(\frac{a}{r}\right)^{12} - 2\left(\frac{a}{r}\right)^6 \right], \quad (20)$$

where ε is the bond energy and a is the equilibrium distance. The potential is smoothly truncated at $a_{\text{cut}} = 1.4a$ using the spline function [36]. Therefore, at least at low temperatures, the interactions are limited to between the nearest neighbors (as in the harmonic model considered above).

Initially, particles have zero displacements and random velocities, directed along the x axis and uniformly distributed in the interval $[-v_0; v_0]$ (in this case, $T_{xx} \neq 0, T_{yy} = T_{zz} = 0$). For small v_0 (at low temperatures), the system is almost linear and it may be approximately described by the harmonic

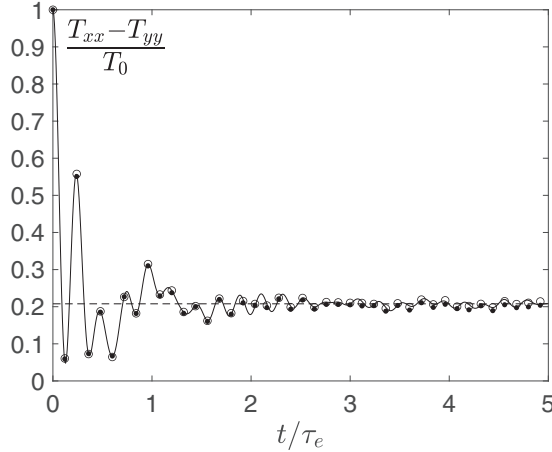


FIG. 5. Equilibration of kinetic temperatures T_{xx} , $T_{yy} = T_{zz}$ in the Lennard-Jones crystal at short times. The analytical solution (12) (solid line) and simulation results for $v_0/v_d = 0.05$ (circles) and 0.25 (black points) are shown. The dashed line shows the equilibrium value, as predicted by the nonequpartition theorem (15).

equations of motion (3), where the stiffness of the spring is equal to $c = \Pi''(0) = 72\varepsilon/a^2$. To investigate the influence of anharmonic effects, we vary the amplitude v_0 of the initial velocities, determining the initial temperature of the system

$$\frac{k_B T_0}{\varepsilon} = \frac{2}{3} \left(\frac{v_0}{v_d} \right)^2, \quad (21)$$

where $v_d = \sqrt{2\varepsilon/m}$ is the dissociation velocity, i.e., the velocity which is required for a particle to leave a potential well of depth ε . In simulations, the difference of temperatures $T_{xx} - T_{yy}$ is calculated.

The simulation results for $v_0/v_d = 0.05, 0.1, 0.25$ are presented in Figs. 5 and 6. Figure 5 shows that at short times the behavior of the temperatures is well described by the harmonic approximation [formula (12)]. The difference of

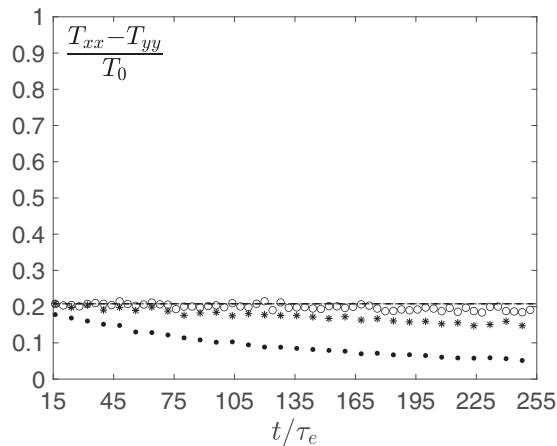


FIG. 6. Equilibration of kinetic temperatures T_{xx} , $T_{yy} = T_{zz}$ in the Lennard-Jones crystal at large times. The analytical solution (12) (solid line) and simulation results for $v_0/v_d = 0.05$ (circles), 0.1 (asterisks), and 0.25 (black points) are shown. The dashed line shows the equilibrium value, as predicted by the nonequpartition theorem (15).

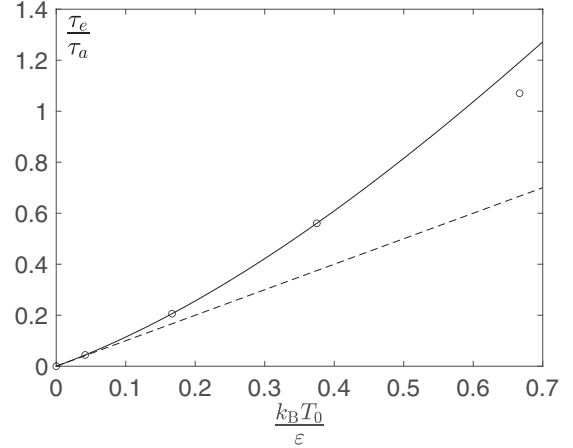


FIG. 7. Temperature dependence of the anharmonic time scale τ_a for $v_0/v_d = 0.25, 0.5, 0.75, 1$. Numerical results (circles), cubic approximation [formula (23), solid line], and linear approximation (dashed line) are shown.

temperatures rapidly reaches the equilibrium value $0.21T_0$, predicted by the nonequpartition theorem (15). At large times, the difference deviates from the equilibrium value and slowly tends to zero (see Fig. 6). The rate of this slow process depends on the initial temperature.

Thus the simulations show that in the anharmonic case the second characteristic time scale, depending on the initial temperature, is present.

B. Dimensional analysis

We determine the anharmonic time scale of the approach to thermal equilibrium using numerical results and the dimensional analysis (see, e.g., Ref. [37]). From this dimensional analysis it follows that the difference $(T_{xx} - T_{yy})/T_0$ depends on three dimensionless parameters t/τ_e , $k_B T_0/\varepsilon$, and a_{cut}/a . In further analysis, we focus on the influence of the first two parameters, while fixed value for the dimensionless cutoff distance $a_{\text{cut}}/a = 1.4$ is used. This value is chosen such that, at least at low temperatures, interactions are limited to between the nearest neighbors.

Simulation results suggest that at large times ($t/\tau_e \gg 1$), the function $(T_{xx} - T_{yy})/T_0$ can be approximated by

$$T_{xx} - T_{yy} = T_0 \Psi(t/\tau_a), \quad \tau_a = \tau_e \varphi(k_B T_0/\varepsilon), \quad (22)$$

where τ_a is the anharmonic time scale, which is dependent on the initial temperature. According to the nonequpartition theorem, $\Psi(0) \approx 0.21$.

We seek an expression for τ_e/τ_a in the form of a series with respect to $k_B T_0/\varepsilon$. The coefficients in the series are calculated by fitting to values of τ_a obtained via numerical simulations. The calculation of τ_a is based on the observation⁴ that the integral of $(T_{xx} - T_{yy})/T_0$ over time from time 0 to $+\infty$ is proportional to τ_a . The resulting dependence of τ_a on the initial temperature is shown in Fig. 7. The numerical results

⁴Linear dependence of the integral on τ_a follows from formula (22).

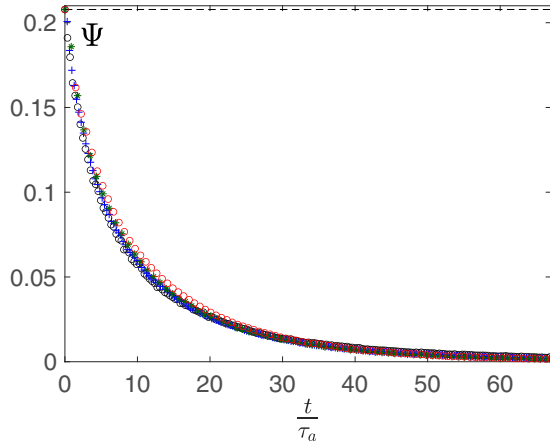


FIG. 8. Equilibration of kinetic temperatures in the Lennard-Jones crystal at different temperatures T_0 [$v_0/v_d = 0.25$ (black circles), $v_0/v_d = 0.5$ (blue crosses), $v_0/v_d = 0.75$ (dark green asterisks), and $v_0/v_d = 1$ (red circles)]. The dashed line shows the equilibrium value, as predicted by the harmonic approximation (15).

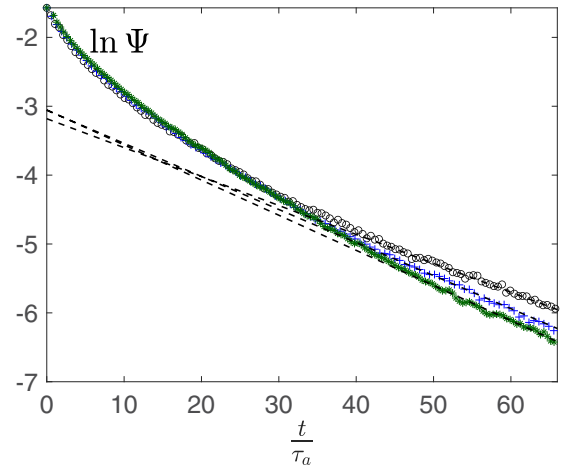


FIG. 9. Equilibration of kinetic temperatures in the Lennard-Jones crystal at different T_0 [$v_0/v_d = 0.25$ (black circles), $v_0/v_d = 0.5$ (blue crosses), and $v_0/v_d = 0.75$ (dark green asterisks)]. The dashed lines correspond to linear approximations at large times.

are fitted to a cubic polynomial

$$\frac{\tau_e}{\tau_a} \approx \frac{k_B T_0}{\varepsilon} + 1.496 \left(\frac{k_B T_0}{\varepsilon} \right)^2 - 0.469 \left(\frac{k_B T_0}{\varepsilon} \right)^3. \quad (23)$$

It can be seen that at low temperatures ($k_B T_0 < 0.05\varepsilon$) the anharmonic time scale is approximately inversely proportional to the initial temperature.

To find the function Ψ , we plot $T_{xx} - T_{yy}$ against the dimensionless time t/τ_a for different values of T_0 (see Fig. 8). Here, τ_a is calculated by formula (23). Figure 8 shows that the simulation results for $v_0/v_d = 0.25, 0.5, 0.75$ practically coincide. Therefore, the assumption of the existence of the universal curve (22), describing equilibration at different temperatures, is satisfied, at least approximately. For $v_0/v_d = 1$, numerical results deviate from the universal curve. This deviation may be caused by the influence of the dimensionless cutoff distance a_{cut}/a . As expected, this parameter, neglected in formula (22), becomes important at high temperatures.

To investigate the behavior of the function Ψ at $t/\tau_a \gg 1$, we plot the time dependence of $\ln \Psi$ (see Fig. 9). The figure shows that at large times Ψ decays exponentially and it may be approximated by

$$\Psi \approx A e^{-Bt/\tau_a}. \quad (24)$$

The parameters A, B in formula (24) are estimated using the data points in Fig. 9 for $t/\tau_a > 45$. These calculations yield $A = 0.044 \pm 0.004$ and $B = 0.046 \pm 0.005$.

Thus, in the anharmonic case, the second time scale, τ_a , is present. This time scale significantly depends on the initial temperature [see formula (23)]. Equilibration at different temperatures is approximately described by the function Ψ , which depends only on the dimensionless time t/τ_a [see formula (22) and Fig. 8].

VI. CONCLUSIONS

We have shown that the equilibration of kinetic temperatures, corresponding to three spatial directions in the anharmonic fcc lattice, has two distinct time scales.

The first time scale is the period of atomic vibrations τ_e . At times of the order of several atomic periods, the approach to equilibrium is accompanied by decaying high frequency oscillations of the temperatures. The oscillations are caused by the redistribution of energy among kinetic and potential forms and among degrees of freedom. These physical processes are described analytically using the harmonic approximation [formula (12)].

It has been shown that oscillations of the average kinetic temperature have six distinct characteristic frequencies (17). Five of these frequencies are such that corresponding group velocities are equal to zero. The remaining frequency corresponds to a discontinuity in the group velocity. It has been shown that, quite unexpectedly, the temperature oscillations decay in time like $1/t$ rather than $1/t^{3/2}$. We suspect that this slow decay may be caused by the Hessian of the dispersion relation being equal to zero at some points. However, additional analysis is required in order to describe the asymptotic behavior of the temperature rigorously.

The second time scale, τ_a , which is present in the anharmonic case only, depends on the initial temperature T_0 . The temperature dependence of the time scale was obtained using molecular dynamics simulations. In particular, it was shown that at low temperatures, τ_a is approximately inversely proportional to T_0 . At the time scale τ_a , the difference of the kinetic temperatures deviates from the equilibrium value, predicted by the harmonic approximation, and monotonically tends to zero. It was shown that this process is approximately described by a function, which depends only on the dimensionless time t/τ_a [see formula (22)]. In other words, equilibration at different temperatures differs only by a time scaling.

The presented analytical results are exact in the case of a spatially uniform distribution of kinetic temperatures. In the case of a nonuniform temperature profile, heat transport should be considered in addition to the transient processes described above. In the harmonic case, relaxation is much faster than heat transport (see, e.g., Ref. [18]). Moreover, relaxation at different spatial points of a harmonic crystal with a nonuniform temperature profile is nearly independent [13,18]. Therefore, in the harmonic case these processes may be considered separately. Our results suggest that, in the weakly anharmonic case, the characteristic time scales of relaxation and heat transfer may be of the same order. Therefore, there may be some mutual influence between these processes. Investigation of this important issue is a subject for future work.

Our results may serve in the development of multicomponent continuum models (see, e.g., Refs. [1,2,8,38,39]). In these models, each component has its own temperature. The behavior of these temperatures is governed by a coupled system of heat transfer equations, where the coupling is caused by energy exchange among the components. Formulas (22)

and (23) can be used in the proper formulation of constitutive relations, describing the coupling. In particular, formula (23) shows how the rate of thermal equilibration depends on temperature. This dependence may be incorporated into the constitutive relations.

Finally, the presented results can be used for the estimation of the range of applicability of the harmonic theory of thermal equilibration [15–22]. We have shown that the theory is applicable at times less than the anharmonic time scale τ_a . For a given initial temperature of the system, τ_a is calculated by formula (23).

ACKNOWLEDGMENTS

The work of V.A.K. was supported by the Russian Foundation for Basic Research, Grant No. 19-01-00633. The work of S.D.L. was supported by the Russian Foundation for Basic Research, Grant No. 20-37-70058. We are deeply grateful to W. G. Hoover and A. M. Krivtsov for useful discussions and to O. Bain for proofreading of the manuscript. The valuable comments of the reviewers are highly appreciated.

-
- [1] J. Casas-Vazquez and D. Jou, Temperature in non-equilibrium states: A review of open problems and current proposals, *Rep. Prog. Phys.* **66**, 1937 (2003).
- [2] N. A. Inogamov, Yu. V. Petrov, V. V. Zhakhovskiy, V. A. Khokhlov, B. J. Demaske, S. I. Ashitkov, K. V. Khishchenko, K. P. Migdal, M. B. Agranat, S. I. Anisimov, V. E. Fortov, and I. I. Oleynik, Two-temperature Thermodynamic and Kinetic Properties of Transition Metals Irradiated by Femtosecond Lasers, AIP Conf. Proc. No. 1464 (AIP, Melville, NY, 2012), p. 593.
- [3] D. der Linde, K. Sokolowski-Tinten, and J. Bialkowski, Laser-solid interaction in the femtosecond time regime, *App. Surf. Sci.* **109**, 1 (1997).
- [4] B. L. Holian, W. G. Hoover, B. Moran, and G. K. Straub, Shock-wave structure via nonequilibrium molecular dynamics and Navier-Stokes continuum mechanics, *Phys. Rev. A* **22**, 2798 (1980).
- [5] O. Kum, W. G. Hoover, and C. G. Hoover, Temperature maxima in stable two-dimensional shock waves, *Phys. Rev. E* **56**, 462 (1997).
- [6] W. G. Hoover and C. G. Hoover, Tensor temperature and shock-wave stability in a strong two-dimensional shock wave, *Phys. Rev. E* **80**, 011128 (2009).
- [7] W. G. Hoover, C. G. Hoover, and K. P. Travis, Shock-wave Compression and Joule-Thomson Expansion, *Phys. Rev. Lett.* **112**, 144504 (2014).
- [8] F. J. Uribe, R. M. Velasco, and L. S. Garcia-Colin, Two kinetic temperature description for shock waves, *Phys. Rev. E* **58**, 3209 (1998).
- [9] S. I. Anisimov, V. V. Zhakhovskii, and V. E. Fortov, Shock wave structure in simple liquids, *JETP Lett.* **65**, 755 (1997).
- [10] V. V. Zhakhovskii, K. Nishihara, and S. I. Anisimov, Shock wave structure in dense gases, *JETP Lett.* **66**, 99 (1997).
- [11] S. Schlamp and B. C. Hathorn, Higher moments of the velocity distribution function in dense-gas shocks, *J. Comput. Phys.* **223**, 305 (2007).
- [12] V. Kannan, A. Dhar, and J. L. Lebowitz, Nonequilibrium stationary state of a harmonic crystal with alternating masses, *Phys. Rev. E* **85**, 041118 (2012).
- [13] V. A. Kuzkin, Unsteady ballistic heat transport in harmonic crystals with polyatomic unit cell, *Continuum Mech. Thermodyn.* **31**, 1573 (2019).
- [14] G. Klein and I. Prigogine, Sur la mecanique statistique des phenomenes irreversibles III., *Physica* **19**, 1053 (1953).
- [15] A. M. Krivtsov, Energy oscillations in a one-dimensional crystal, *Dokl. Phys.* **59**, 427 (2014).
- [16] M. B. Babenkov, A. M. Krivtsov, and D. V. Tsvetkov, Energy oscillations in a one-dimensional harmonic crystal on an elastic substrate, *Phys. Mesomech.* **19**, 282 (2016).
- [17] V. A. Kuzkin and A. M. Krivtsov, An analytical description of transient thermal processes in harmonic crystals, *Phys. Solid State* **59**, 1051 (2017).
- [18] V. A. Kuzkin and A. M. Krivtsov, Fast and slow thermal processes in harmonic scalar lattices, *J. Phys.: Condens. Matter* **29**, 505401 (2017).
- [19] V. A. Kuzkin, Thermal equilibration in infinite harmonic crystals, *Continuum Mech. Thermodyn.* **31**, 1401 (2019).
- [20] S. N. Gavrilov and A. M. Krivtsov, Thermal equilibration in a one-dimensional damped harmonic crystal, *Phys. Rev. E* **100**, 022117 (2019).
- [21] A. S. Murachev, A. M. Krivtsov, and D. V. Tsvetkov, Thermal echo in a one-dimensional harmonic crystal, *J. Phys.: Condens. Matter* **31** (2019).
- [22] I. E. Berinskii and V. A. Kuzkin, Equilibration of energies in a two-dimensional harmonic graphene lattice, *Philos. Trans. R. Soc. A* **378**, 20190114 (2019).
- [23] V. A. Tsaplin and V. A. Kuzkin, Temperature oscillations in harmonic triangular lattice with random initial velocities, *Lett. Mater.* **8**, 16 (2018).
- [24] M. V. Fedoryuk, The stationary phase method and pseudodifferential operators, *Russian Math. Surv.* **26**, 65 (1971) (in Russian).

- [25] R. Wong, *Asymptotic Approximation of Integrals* (Academic Press, New York, 1989).
- [26] V. A. Kuzkin and A. M. Krivtsov, Ballistic resonance and thermalization in Fermi-Pasta-Ulam-Tsingou chain at finite temperature, *Phys. Rev. E* **101**, 042209 (2020).
- [27] I. Prigogine and F. Henin, On the general theory of the approach to equilibrium. I. Interacting normal modes, *J. Math. Phys.* **1**, 349 (1960).
- [28] E. Fermi, P. Pasta, S. Ulam, and M. Tsingou, Studies of nonlinear problems, United States: N. p., 1955, doi:10.2172/4376203.
- [29] T. Dauxois, Fermi, Pasta, Ulam, and a mysterious lady, *Phys. Today* **61**, 55 (2008).
- [30] *The Fermi-Pasta-Ulam Problem: A Status Report*, edited by G. Gallavotti, Lecture Notes in Physics Vol. 728 (Springer, Berlin, 2008).
- [31] G. P. Berman and F. M. Izrailev, The Fermi-Pasta-Ulam problem: Fifty years of progress, *Chaos* **15**, 015104 (2005).
- [32] M. Onorato, L. Vozella, D. Proment, and Y. V. Lvov, Route to thermalization in the α -Fermi-Pasta-Ulam system, *Proc. Natl. Acad. Sci. USA* **112**, 4208 (2015).
- [33] S. G. Das, A. Dhar, K. Saito, C. B. Mendl, and H. Spohn, Numerical test of hydrodynamic fluctuation theory in the Fermi-Pasta-Ulam chain, *Phys. Rev. E* **90**, 012124 (2014).
- [34] S. V. Dmitriev, A. A. Sukhorukov, A. I. Pshenichnyuk, L. Z. Khadeeva, A. M. Iskandarov, and Y. S. Kivshar, Anti-Fermi-Pasta-Ulam energy recursion in diatomic lattices at low energy densities, *Phys. Rev. B* **80**, 094302 (2009).
- [35] E. A. Podolskaya and A. M. Krivtsov, Description of the geometry of crystals with a hexagonal close packed structure based on pair interaction potentials, *Phys. Solid State* **54**, 1408 (2012).
- [36] A. A. Le-Zakharov and A. M. Krivtsov, Molecular dynamics investigation of heat conduction in crystals with defects, *Dokl. Phys.* **53**, 261 (2008).
- [37] G. I. Barenblatt, *Scaling, Self-Similarity, and Intermediate Asymptotics* (Cambridge University Press, Cambridge, UK, 1996).
- [38] D. A. Indeitsev, V. N. Naumov, B. N. Semenov, and A. K. Belyaev, Thermoelastic waves in a continuum with complex structure, *Z. Angew. Math. Mech.* **89**, 279 (2009).
- [39] B. L. Holian, A. Mareschal, and R. Ravelo, Test of a new heat-flow equation for dense-fluid shock waves, *J. Chem. Phys.* **133**, 114502 (2010).